



# New insights into the structural development and shortening of the southern Jasmund Glacitectonic Complex (Rügen, Germany) based on balanced cross sections

Anna Gehrman<sup>1</sup> · Stig A. Schack Pedersen<sup>2</sup> · Martin Meschede<sup>1</sup>

Received: 15 December 2021 / Accepted: 2 June 2022 / Published online: 24 June 2022  
© The Author(s) 2022

## Abstract

Late Pleistocene glacitectonism at the southern Scandinavian Ice Sheet margin caused folding and thrusting of Upper Cretaceous chalk layers and Pleistocene glacial deposits in parts of the southwestern Baltic Sea area in Europe. Beside Møns Klint (SE Denmark), the Jasmund Glacitectonic Complex (JGC) on Rügen Island (NE Germany) is a similar striking example of glacitectonic deformation creating large composite ridges. In spite of a long research history and new results from modern datasets, the structural development of the JGC is still poorly understood, especially the detailed evolution of the southern JGC and its relationship to the northern JGC remain enigmatic. In this contribution, we demonstrate how the understanding of the JGC benefits from the application of established structural geological methods comprehending the formation of fold-and-thrust belts. The methods include cross-section balancing of the eastern coast (southern JGC) and quantification of the amount of folding and faulting. The proposed geometric model shows the current fold-and-thrust stack of glacially deformed sedimentary strata ca. 5720 m in length evolved by shortening from the original length (11,230 m) by 5510 m (49.1%). We present a spatial and temporal development of fault-related folding with a transition from detachment folds through fault-propagation folds to fault-bend folds. Together with morphological information from a digital elevation model, the thrust faults mapped in the cliff section are mainly inclined towards the S to SW and imply that a local glacier push occurred from the south. These results highlight the complexity and individual architecture of the JGC when compared to other Pleistocene and modern glacitectonic complexes. Resolving its structural development provides new insight into the deformation history and shortening of this spectacular glacitectonic complex lying in the southwestern Baltic Sea region.

**Keywords** Late Pleistocene · Glacitectonics · Scandinavian Ice Sheet · Thin-skinned thrust tectonics · Fault-related folding · Structural analysis · Balanced cross sections

## Introduction

Since Johnstrup (1874) compared the elevated Cretaceous chalk strata exposed at Møns Klint on Møn Island in SE Denmark and the Jasmund cliff on Rügen Island in NE Germany, the concept of glacier activity for the formation of the chalk cliffs in the southern Baltic Sea region has been generally accepted. Slater (1927) introduced a model for glacitectonics and Gripp (1947), who studied glacitectonics in modern glacial settings on Svalbard in 1926, provided a glacial morphological investigation that highlighted the similarity between the Jasmund and Møns Klint sites. It is well known that the Jasmund and Møn cliff sections have an almost identical structural framework with Upper Cretaceous Maastrichtian chalk strata displaying steeply-inclined bedding intersected by vegetation-rich gorges filled with

✉ Anna Gehrman  
gehrman.anna@outlook.com

Stig A. Schack Pedersen  
sasp@geus.dk

Martin Meschede  
meschede@uni-greifswald.de

<sup>1</sup> Institute for Geography and Geology, University of Greifswald, Friedrich-Ludwig-Jahn-Straße 17a, 17487 Greifswald, Germany

<sup>2</sup> Geological Survey of Denmark and Greenland (GEUS), Øster Voldgade 10, 1350 Copenhagen, Denmark

Pleistocene deposits. The kineto-stratigraphical method applied by Berthelsen (1978) to glacial geology inspired the study of glacetectonics on Møn. Pedersen (2000) introduced the concept of superimposed deformation in glacetectonics, and the structural framework of Møns Klint could be resolved during research of chalk cliff collapse in the years 2002–2015 (Pedersen and Møller 2004; Pedersen and Gravesen 2009; Pedersen 2014). Structural analysis of Jasmund was conducted by Ludwig (1954/55, 2011), Steinich (1972), Groth (2003), Kenzler et al. (2010), and Gehrmann et al. (2017).

Understanding the structural development of the Jasmund Glacitectonic Complex (JGC) has been challenging for many years and a number of structural models have been presented (e.g. Ludwig 1954/55, 2011; Steinich 1972; Groth 2003). However, modern data and advanced imaging methods have provided a wide range of possibilities to reassess and enhance existing interpretations. Gehrmann and Harding (2018) proposed a new model for the glacetectonic development of the JGC in various phases characterised by different glacier-flow directions based on geomorphological analyses of a LiDAR-based digital elevation model (DEM). However, the detailed structural development of the southern JGC and its relationship to the northern JGC remain enigmatic. Thus, this paper aims at unravelling the glacetectonic evolution and to quantify the deformation in the southern JGC that was affected by a sequence of several local glacier-lobe advances of the southern Scandinavian Ice Sheet margin.

Our specific research questions addressed are the following: (i) Is the JGC comparable to other Pleistocene and modern glacetectonic complexes? (ii) Was the southern JGC formed after the northern JGC by a local glacier push from SE as suggested in the geomorphologically based model presented by Gehrmann and Harding (2018)? To answer these questions, we demonstrate how the investigation of glacetectonic complexes benefits from the application of established structural geology methods such as cross-section balancing and correlation of geomorphology with the 2D structure. Such complexes are representative of soft-sediment deformation by glacier activity on a much smaller scale than large orogenic belts, where cross-section balancing was first applied in the 1960–1980s (e.g. Dahlstrom 1969; Suppe 1985). This approach has already been successfully applied to other glacetectonic settings (Croot 1987, 1988; Boulton et al. 1999; Pedersen 2005; Benediktsson et al. 2010; Lohrberg et al. 2021).

## Geological setting

The JGC is situated in the northeastern part of Rügen Island (North Germany) along the southwestern coastline of the Baltic Sea (Fig. 1a, b). The glacial geomorphology of the

JGC has been described and analysed in detail by Gehrmann and Harding (2018) showing a sequence of SW–NE-trending composite ridges in the southern part (southern JGC) and approximately NW–SE-trending composite ridges in the north (northern JGC) (Fig. 1c).

The glacetectonic configuration of Jasmund represents a fold-and-thrust belt similar to the Danish glacetectonic complexes Møns Klint and Rubjerg Knude (Pedersen 2000, 2005; Gehrmann et al. 2019). Upper Cretaceous (Maastrichtian) chalk layers as well as unconsolidated Pleistocene glacial deposits are deformed resulting in a number of folds and associated thrusts (Credner 1893; Gripp 1947; von Bülow 1955; Groth 2003; Ludwig 2011). The glacial sediments, lying para-conformably on top of the Maastrichtian chalk, are exposed in large synclines of the JGC, mainly cut by thrust faults at the southern fold limbs. The faults in the southeastern and eastern cliff sections are generally inclined towards S–SW, while the thrust faults exposed at the northern cliff coast dip towards NNE/NE (see Steinich 1972; Ludwig 2005, 2011; Müller and Obst 2006). The glacial deposits are subdivided into at least three tills (M1–M3) that are separated and overlain by units of interbedded gravel, sand, and clay (I1 and I2). The two older tills M1 and M2 together with the intercalated glacial successions are located within the glacetectonic synclines. The youngest till is exposed at the top of the cliff, where it lies unconformably upon a major erosion surface, which truncates the underlying glacetectonised sequence (Jaekel 1917; Panzig 1995; Ludwig 2011).

The older M1 till is commonly regarded as deposited during the Saalian glaciation (Marine Isotope Stage MIS 6; Panzig 1995; Müller and Obst 2006). No unequivocal Eemian aged sediments (MIS 5e) have been identified in the Jasmund cliff sections (Steinich 1992; Ludwig 2006). The majority of the Pleistocene sedimentary record (I1, M2, I2 and M3) on the Jasmund Peninsula was deposited during the Weichselian glaciation when the Scandinavian Ice Sheet (SIS) extended southwards across the Baltic Sea and into northern Europe. In this part of the Baltic Sea, the Weichselian glaciation was divided into three ice advances – the Brandenburg/Frankfurt phase (W1, < 24 ka BP), the Pomeranian phase (W2, 17.6 ka BP), and the Mecklenburg phase (W3, 17–15 ka BP) (Katzung and Müller 2004; Müller 2004; Litt et al. 2007; Janke and Niedermeyer 2011; Rinterknecht et al. 2014). These three phases resulted in the deposition of regionally extensive till sheets intercalated by glacialustrine to glacialfluvial sequences (Panzig 1995; Ludwig 2005; Müller and Obst 2006; Janke and Niedermeyer 2011). The formation of the JGC post-dated the deposition of the M2 unit corresponding to the Brandenburg/Frankfurt W1 advance (Gehrmann et al. 2017; Gehrmann and Harding 2018). Consequently, glacetectonism of the JGC probably occurred after the Last Glacial Maximum (LGM, MIS 2) with folding and thrusting occurring in response

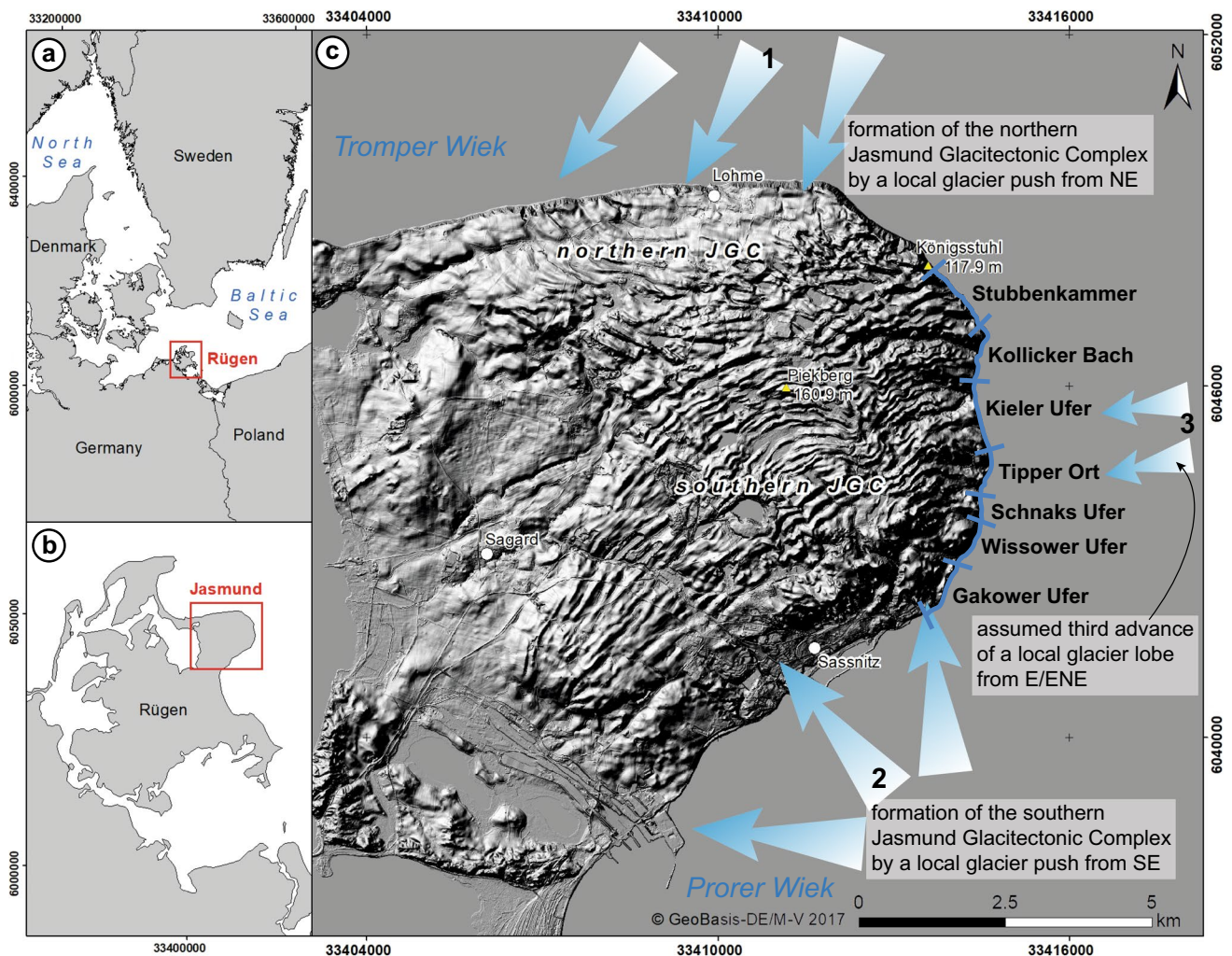


**Fig. 1** Position and genetic model of the Jasmund Glacitectonic Complex (JGC) related to different advances of glacier lobes at the southern Scandinavian Ice Sheet margin during the late Weichelian; coordinate system: ETRS 1989 UTM Zone 33 N (zE-N). **a** Location of Rügen Island in the southwestern Baltic Sea. **b** Position of the Jasmund Peninsula in the northeast of Rügen Island. **c** Digital elevation model (10 times exaggerated, hillshade, LiDAR data provided by the

LAiV M-V) of the Jasmund Peninsula, which shows the surficial separation into the northern and southern JGC. The eastern cliff district from Sassnitz to the Königsstuhl is separated into sections and provided with the labels used in this paper. Three proposed local glacier advances of the late Weichelian indicating different flow directions are visualised (based on the model suggested by Gehrman and Harding 2018)

to a re-advance of the Scandinavian Ice Sheet during the Pomeranian W2 phase (around 18.5–16.0 ka) (Groth 2003; Müller and Obst 2006; Kenzler et al. 2022). On the Danish side of the Baltic Sea, these glaciodynamic events correspond to the main ice advance at the LGM, which settled the Main Stationary Line and deposited the Mid Danish Till Formation and the two late Weichselian Young Baltic Ice advances (Houmark-Nielsen 1987, 2007; Pedersen 2014).

Several models have been proposed during the last decades to explain the complicated structural evolution of the JGC, for instance Groth (2003) and Ludwig (1954/55, 2011). A recently published model by Gehrman and Harding (2018) is based on more recent data and methods, such as the spatial analysis of LiDAR-based digital

elevation models (DEM). The most recent models suggest a polyphase structural development for the JGC in the late Weichselian (Pomeranian phase, W2), comprising of at least two stages. The first evolutionary stage was characterised by a local NE-to-SW push by a lobe of the Scandinavian Ice Sheet (SIS) forming the northern JGC. In the second evolutionary stage, the southern JGC was formed. The orientation of the ridge crests (SW–NE) differs from those of the northern JGC (NW–SE), as a lobe of the SIS might have pushed the local deposits from the SE (Fig. 1c). Gehrman and Harding (2018) suggested a third evolutionary stage with a local ice push from the E/ENE. The existence of a till complex on top of the glaci-tectonised sequence in the northern and southern JGC is

an indicator that the ice eventually overrode the complex, at least along its marginal zones.

## Methodology

### Construction of geological cross sections

For the understanding of the tectonic architecture and structural development of the southern JGC, we performed a detailed structural analysis of the coastal sections. Geological cross sections were digitally constructed based on detailed geological profiles of Jasmund's southeastern and eastern coast as presented by Steinich (1972). We recorded the cliff sections by detailed field examination and via photographic imaging of the cliff sections taken by boat 500 m from the coastline and with the help of a multicopter (DJI Mavic 2 Pro). Included in the study was the analysis of a LiDAR-based DEM of Jasmund, which was provided by the Landesamt für innere Verwaltung Mecklenburg-Vorpommern, Schwerin, Germany, and optimized for structural analysis and interpretation. The cliff sections were

separated into seven related cross sections including at least 23 thrust sheets (S01 to S23, Steinich 1972). The sections (from S to N) were labelled as Gakower Ufer (S01–S03), Wissower Ufer (S04), Schnaks Ufer (S05 – S07), Tipper Ort (S08–S10), Kieler Ufer (S11–S16), Kollicker Bach (S17–S19), and Stubbenkammer (S20–S23), respectively (Figs. 1, 3 to 5).

The software Move 2017.1 (Midland Valley Exploration Ltd. 2017) was used to construct balanced cross sections. For digitisation, the cross sections from Steinich (1972) were inserted into previously constructed section traces containing information on the cliff-face orientation. The flint layers in the chalk unit were used as individual marker horizons (F01–F66) providing the detailed structural information and reliable interpretation (Fig. 2). Thickness information could be derived from the well-exposed flint layers in the cross section S08 (see Steinich 1972). However, the thickness between the individual flint layers changes across the entire eastern cliff, so the values needed to be adapted for the particular sections. The top of the chalk unit is labelled as “chalk top”. The Pleistocene beds are traditionally labelled as M1, I1, M2, and I2. Simplifications to the

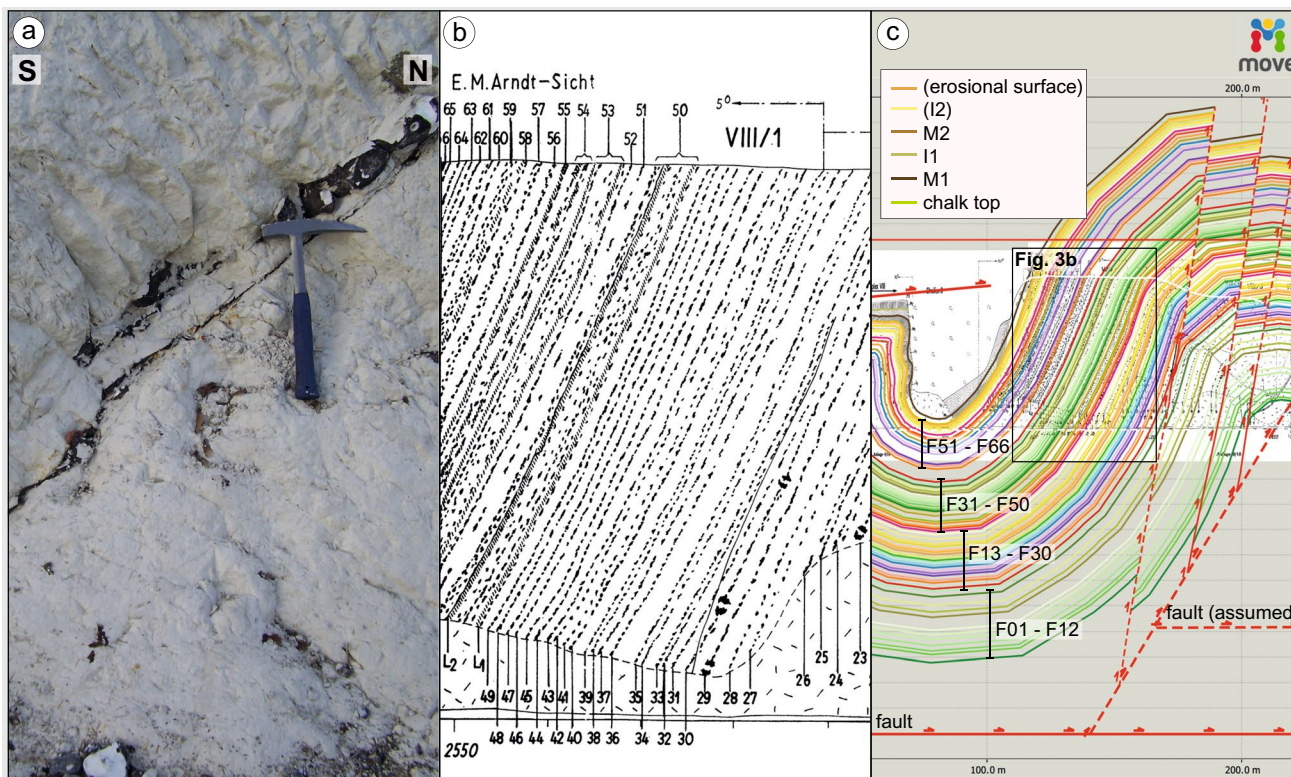


**Fig. 2** Concept of visualisation and digitisation of flint layers at the exemplary outcrop Ernst–Moritz–Arndt–Sicht (S08/TO<sub>3</sub>) in the Tipper Ort Section. The orientation of the cross section S08 is SSW–NNE. **a** Example of a moderately inclined flint layer within the Cretaceous chalk; 54°31′37.4″N 13°40′20.6″E. **b** Extract of the original

geological cross section mapped by Steinich (1972) showing the Cretaceous flint layers of thrust sheet S08. **c** Digitised thrust sheet S08 with the original map in the background. The coloured horizons indicate flint bands and the top of reliable beds. The flint-band numbers of F01 to F66 have been adopted from Steinich (1972)

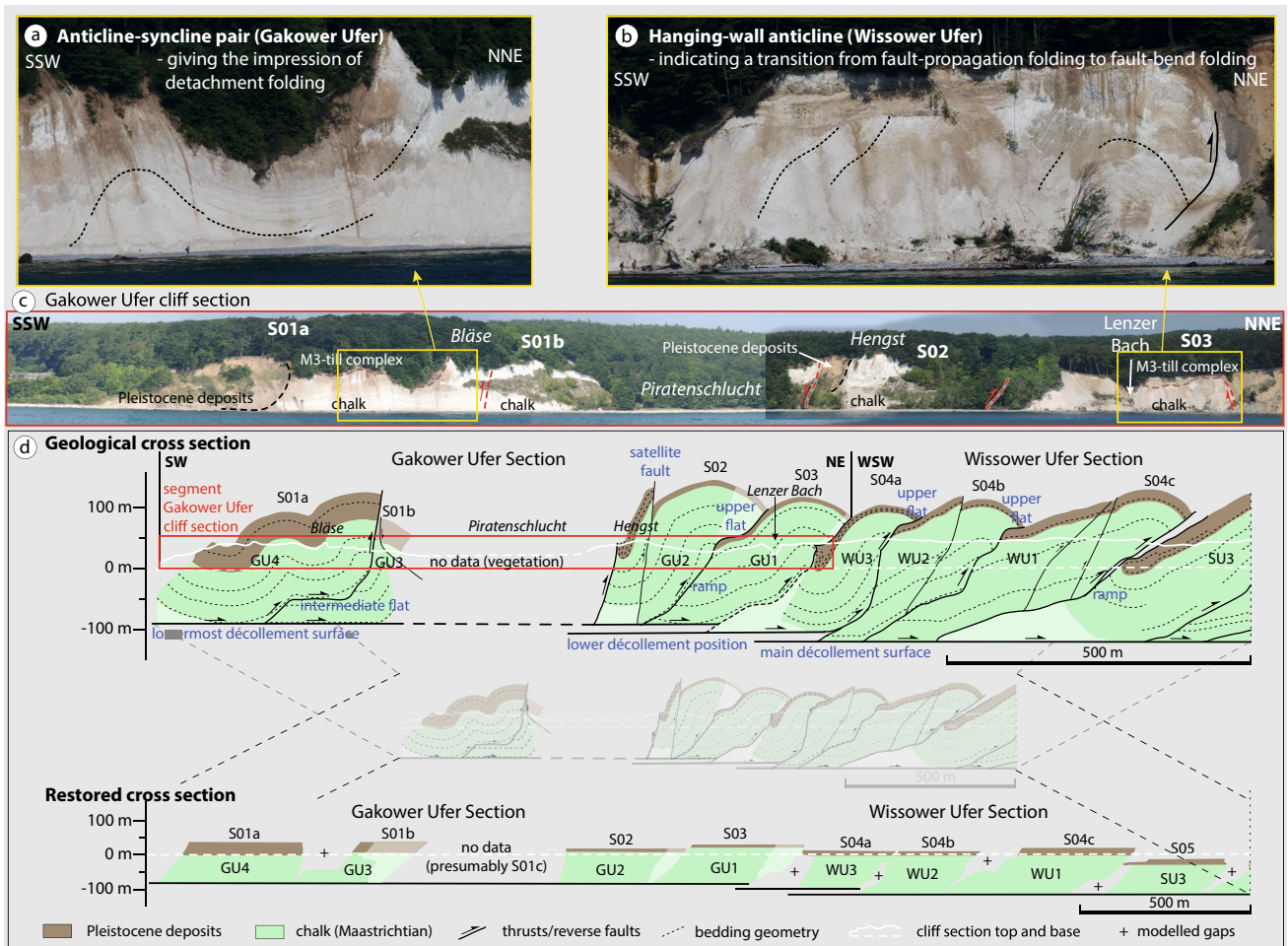


**Fig. 3** Structural configuration of the Gakower and Wissower Ufer Section. The abbreviations S01a to S05 are adopted from Steinich (1972). **a** Exemplary anticline-syncline pair at the Gakower Ufer. **b** Exemplary hanging-wall anticline of the Wissower Ufer. **c** Panoramic

photo of the Gakower Ufer Section. **d** Geological cross section of the Gakower and Wissower Ufer Section together with the restored cross section below

bedding structure were made to ease modelling. Thus, local geometrical adjustments to the original cross sections from Steinich (1972) were employed, based on field observations of parasitic folds and smaller faults present in, for example, the thrust sheet S04 of the Wissower Ufer or the S18 of the Kollicker Bach Section. Prior to structural modelling, each digitised cross section was projected to show its true profile plane perpendicular to the regional strike of the major thrust faults and to the main orientation of the local ridges and corresponding valleys in the DEM. Consequently, the azimuth of each section corresponds to the direction of tectonic transport.

Based on the rules of fault-related folding (e.g. the ramp geometry corresponds to the backlimb dip of the hanging-wall anticline), we interpreted the geometry beyond the top and bottom lines of each cross section. For horizon construction, the appointed stratigraphy and known horizons from the mapped cliff sections were used as template horizons

(Fig. 2c). The parallel (bisector) construction method was applied in Move, which assumes parallel folds. The software-based cross-section construction facilitated the description of bed shapes and fold structures, measurement of fault and bed orientations, classification of existing thrust systems, but also the definition of sedimentary units. The orientation data were given as dip direction and dip angle.

**Restoration of geological cross sections**

To aid understanding of the structural configuration and development of the southern Jasmund Glacitectonic Complex, we restored the geological cross sections including a quantitative partitioning of deformation into folding and faulting portions. The technique of cross-section restoration in glacial environments is known to be inherently more complex than in orogenic fold-and-thrust belts as e.g., the glacitectonic disturbances are too complex (Benediktsson

et al. 2010). Nevertheless, cross-section balancing has been an increasingly applied method in glacial environments. This was demonstrated for instance by Croot (1987, 1988), Boulton et al. (1999), Pedersen (2005), Benediktsson et al. (2010), Winsemann et al. (2020), and Lohrberg et al. (2021). Regarding to the structural evolution of a fold-and-thrust belt, balancing works backwards from the distal to the proximal deformation area. Thus, the deformational features of the Stubbenkammer Section (S20–S23) closest to the foreland of the southern JGC were the first to be restored and those of the Gakower Ufer Section (S01–S03) closest to the hinterland were restored last. This involved restoring the single sections of Stubbenkammer (SK), Kollicker Bach (KB), Kieler Ufer (KU), Tipper Ort (TO), Schnaks Ufer (SU), Wissower Ufer (WU) and Gakower Ufer (GU) in the order given (Figs. 3, 4, 5). Each thrust sheet within these areas was restored to its original geometry. In the end, the single restored blocks were then reassembled. The specific

approach was adapted from the restoration workflow of the Wheeler Ridge anticline in California, USA (Mueller and Suppe 1997).

The restoration process was undertaken in several stages using different algorithms and bedding geometries to obtain the best-fit interpretation for each section. The favoured solution was then used for shortening calculations and further interpretation. Within the scope of the restoration, the individual thrust sheets (S01–S23) were re-named according to the single sections mentioned above and the chronology of restoration, always starting at the most distal part and ending at the most proximal part. Thus, for instance S17, S18, and S19 of the Kollicker Bach Section were labelled as KB3, KB2, and KB1 (see Figs. 4 and 5). The amount of horizontal shortening could be determined by calculating the difference between the length of the deformed and undeformed beds. Restoration and measurements were performed with the software Move and the supplementary

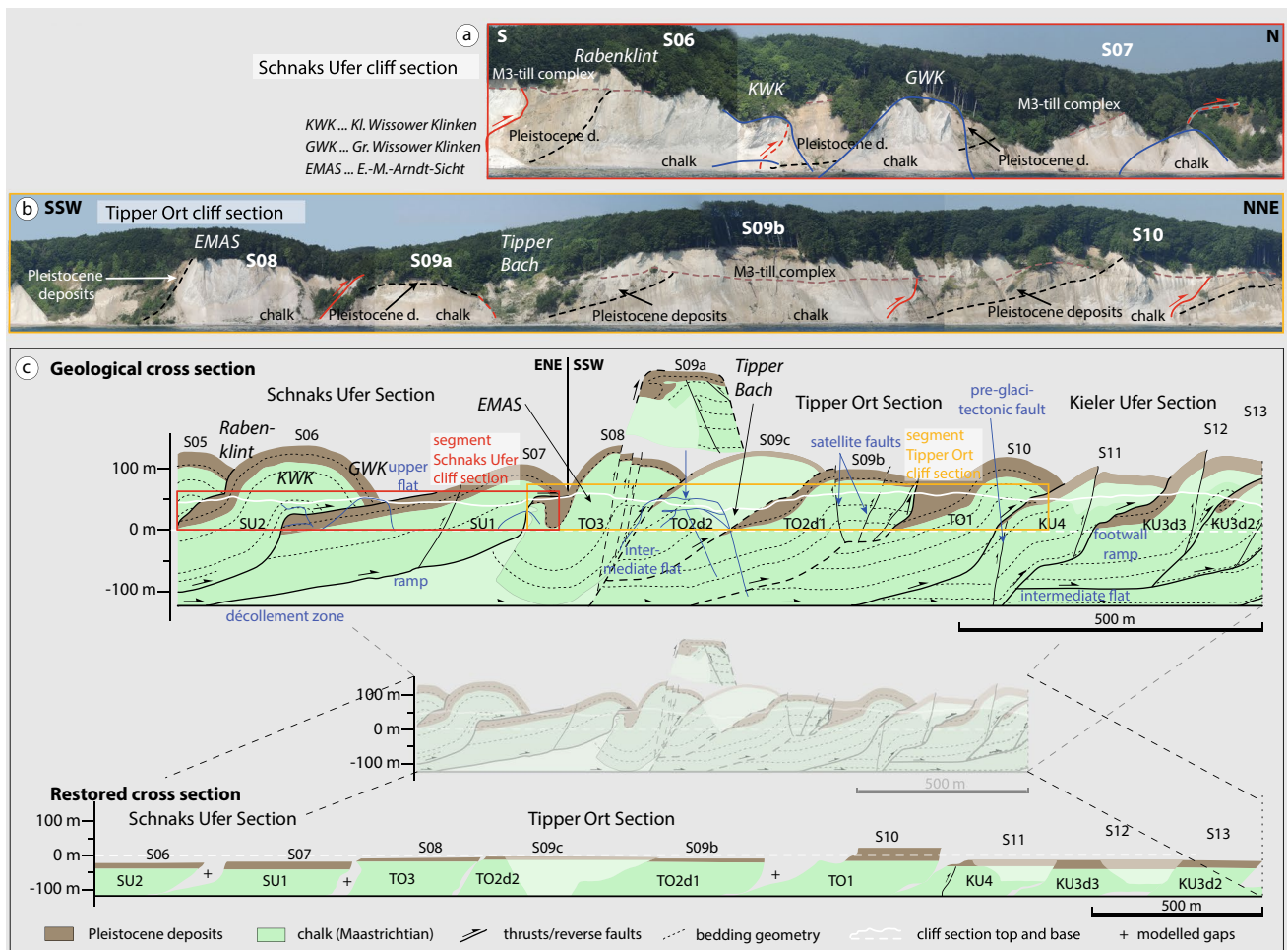


**Fig. 4** Structural configuration of the Schnaks Ufer, Tipper Ort, and the trailing part of the Kieler Ufer Section. The abbreviations S05 to S13 are adopted from Steinich (1972). **a** Panoramic photo of the Schnaks Ufer cliff section. **b** Panoramic photo of the Tipper Ort cliff

section. **c** Geological cross section of the Schnaks Ufer, Tipper Ort, and the trailing part of the Kieler Ufer Section together with the restored cross section below

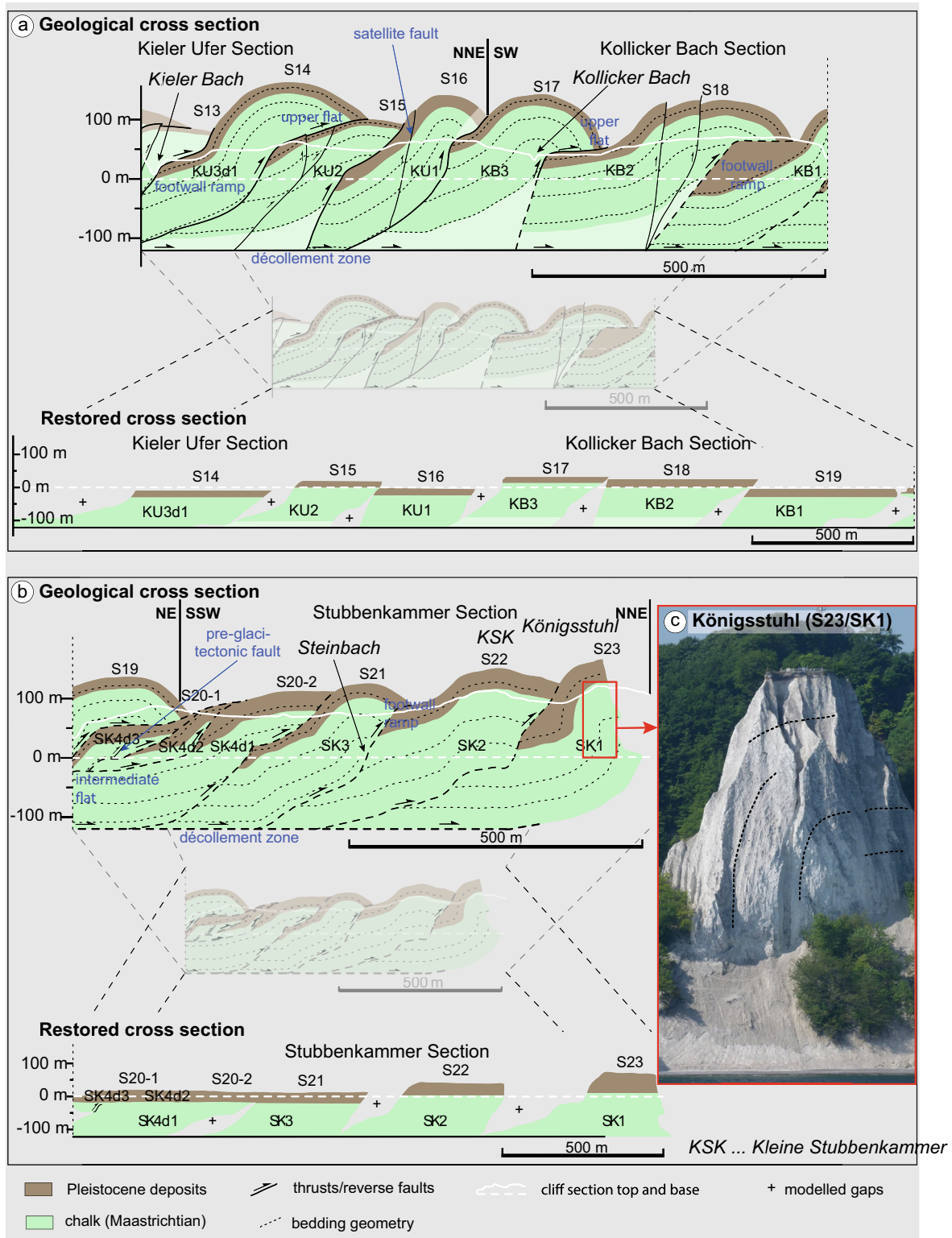


**Fig. 5** Structural configuration of the frontal part of the Kieler Ufer Section, the Kollicker Bach and Stubbenkammer Section. The abbreviations S13 to S23 are adopted from Steinich (1972). **a** Geological cross section of the Kieler Ufer and Kollicker Bach Section together with the restored cross section below. **b** Geological cross section of

the Stubbenkammer Section together with the restored cross section below. **c** Photo of the Königsstuhl representing the frontal part of the Stubbenkammer Section; visualisation of the bedding geometry indicated by the flint layers

module 2D Kinematic Modelling. As a first restoration step, the *Fault Parallel Flow* algorithm (Egan et al. 1997; Kane et al. 1997; Ziesch et al., 2014) of the 2D Move on Fault workflow was applied to undeform the youngest reverse faults in the hanging-wall anticlines of certain thrust sheets. The 2D Unfolding workflow of Move was used to further restore each thrust sheet. We tested both the *Flexural Slip* and *Line Length* algorithm of this workflow. The algorithm *Line Length* unfolds deformed horizons to perfectly straight lines and maintains line length. The *Flexural Slip* algorithm maintains bed thickness variations and line length of the template horizon and of passive objects parallel to that. The line-length unfolded thrust sheets were used for horizontal-shortening calculations.

Fold-thrust systems undergo shortening by the three complementary deformation mechanisms of layer-parallel shortening, buckle folding and faulting (e.g., Dixon and Liu 1992; Noble and Dixon 2011). Thus, our structural analysis includes partitioning of the deformation into these mechanisms to differentiate between fold-dominated, fold-thrust-dominated and thrust-dominated domains (see Boulton et al. 1999). In the glacetectonic setting of fault-related folding proposed for the southern JGC, we separated the amount of shortening into folding and faulting portions. However, layer-parallel shortening was not further elaborated and is included in the shortening amount by faulting (as translation along décollement and thrust faults). For each of the seven sections, the total minimum shortening was placed on a level of 100%. Absolute values of the horizontal shortening by folding were calculated by subtracting the length of the deformed cross-section from the length of the restored cross section. The percentage of the folding part was calculated based on the absolute value of bulk shortening. To determine the absolute value of the translation, the difference between the absolute minimum shortening and the absolute folding value was calculated and cross-checked with the measurements of the distance between the bed-tip positions in the constructed and restored cross section (displacement along the décollement and individual thrust faults).

## Results

### Model-based structural description

The southern JGC represents a fold-and-thrust system. It is a large imbricate fan with at least 21 individual thrust sheets and three duplex stacks (Figs. 3, 4, 5). The décollement zone is located at a depth of ca. 120 m below sea level (b. s. l.) However, the position changes to 105 m b. s. l. (WU3) and 90 m b. s. l. (GU1) in the proximal zone. The dimensions and key structural characteristics of the individual thrust sheets are summarised in Table 1. The model proposed here

represents a simplification of the cross sections given by Steinich (1972).

The proximal part of the southern JGC includes the sections Gakower, Wissower, and Schnaks Ufer, while the Schnaks Ufer Section constitutes a transition zone between the proximal and central part. The southernmost part is the Gakower Ufer Section, which contains at least four individual thrust sheets (Fig. 3). Based on Keilhack (1912), Jaekel (1917), and Steinich (1972), they are labelled as GU4, GU3, GU2, and GU1. The abbreviations in parentheses are the new suggestions of tectonic units presented here. The Gakower Ufer Section shows folds by an anticline-syncline pair in GU4 (Fig. 3a). The fold axial planes have been determined in the model to moderately dip to NE (040/63, 040/73, 040/63, 040/84). At first view, these structures are akin to detachment folds. Furthermore, the folds rest on an intermediate flat at ca. 50 m b. s. l. when considering the modelled cross section (Fig. 3d). The best-fit model of the Wissower Ufer Section shows a relatively simple imbricate fan with three individual thrust sheets WU3, WU2, and WU1 (Fig. 3). Based on field observations, modelling, and detailed macro- and microtectonic descriptions, a thrust steeply dipping towards the WSW (245/85) is suggested for the WU3/WU1-boundary (Mehlhorn et al. 2019). Down towards the décollement zone at 105 m b. s. l. it becomes less steeply inclined in a listric manner (245/46, 245/25) (Tab. 1). The structural configuration at the southern part of the Wissower Ufer Section may represent a transition from fault-propagation folding to fault-bend folding (Fig. 3b).

The Schnaks Ufer Section shows an imbricate fan with three thrust sheets SU3, SU2, and SU1 that contain internal hanging-wall anticlines. The southern sheet SU3 bounding the frontal thrust of the Wissower Ufer Section shows a distinct footwall syncline indicative of true fault-bend folds (Figs. 3d and 4). Thrust sheet SU1 constructed as a long gently inclined thrust sheet, has been significantly simplified to perform the modelling process. The central zone of the southern JGC includes the Tipper Ort and Kieler Ufer Section (Figs. 4 and 5). The Tipper Ort Section shows an imbricate thrust system with two thrust sheets TO3 and TO1, but a duplex stack in between them—TO2d1 and TO2d2 (Fig. 4c). According to Pedersen (2005) and Gehrman et al. (2019), duplex segments are simply differentiated by their shape into an L-, S-, and G-type and they indicate zones of strong contraction. The three types are labelled according to their general shapes as follows: an L-structure looks like the latin letter L, an S-structure like an S and a G-structure like the Greek capital letter gamma ( $\Gamma$ ). Both the lower (TO2d1) and the upper (TO2d2) duplex segment were determined to be S-type elements. The ledge “S09a” (see Steinich 1972) removed from the model for simplification, seems to have experienced complicated deformation, as assumed for the GWK and KWK in SU1. The frontal ramp of the Tipper Ort



**Table 1** Summary of the structural features of the individual sections and thrust sheets in the southern Jasmund Glacitectonic Complex

Sections		Highest cross-section elevation (m)	Thrust sheets	Total length (m)	Total bed thickness (F01—youngest bed top) (m)	Orientation of the frontal ramp (base to top, dip direction/dip)	Youngest flint band	
Gakower Ufer section	S	145	S01a	GU4	368	≤ 125	220/42— 220/52— 220/81	(F50); F38
			S01b	GU3	≥ 224	–	–	(F50); F46
			(S01c)	–	–	–	220/76	–
			S02	GU2	283	ca. 90—112	220/22— 220/49— 220/72	F50
Wissower Ufer Section		119	S03	GU1	338	115	245/25— 245/46— 245/85	(F53)
			S04a	WU3	232	114	250/77—250/53	F53
			S04b	WU2	366	134—153	225/40	F54
			S04c	WU1	499	135	260/22	F54
Schnaks Ufer Section		137	S05	SU3	699	(187)—126	225/27— 225/71— 220/47	F56
			S06	SU2	490	132—105	245/12—245/50	F56
			S07	SU1	745	120	205/15—205/67	F54
			S08	TO3	326 (689)	110	210/50	F66
Tipper Ort Section		135	S09a	–	–	(132)	–	(F64)
			S09b	TO2d2	526	109—114	210/35	F56
			S09c	TO2d1	357	107	215/22—215/61	F51/F56
			S10	TO1	566	≤ 160	205/16— 205/59— 205/38	F54
Kieler Ufer Section		166	S11	KU4	478	≤ 116	225/46— 225/13— 225/61	F54
			S12	KU3d3	506	106 (from F01); 131	190/45	F54
			S13	KU3d2	315	≤ 108	220/12—220/53	F54
			S14	KU3d1	820	≤ 111	210/21— 210/60— 210/24	F54
Kollicker Bach Section		134	S15	KU2	427 (≤ 477)	≤ 128 (F01)	205/65—205/38	F54
			S16	KU1	294	122—ca. 113	210/38—210/79	F54
			S17	KB3	425	125—140	235/72	F54
			S18	KB2	496	114—124	200/50	(F54)
Stubbenkammer Section		147	S19	KB1	502	133—79	210/35	F54
			S20-1	SK4d2/SK4d3	307	76	210/56	(F50)
			S20-2	SK4d1	653	96—79	210/45 to 210/28	F53
			S21	SK3	465	120—125	185/28—185/56	F57
	N		S22	SK2	513	165	185/18—185/57	F63
			S23	SK1	547	164—175	–	(F59)

Values in parentheses are subject to debate or not fully clear. The italic values are not fully clear due to an incomplete stratigraphy

Section (TO1) dips gently to the SSW when it emerges from the décollement zone (205/16). Then it changes to a more moderate inclination immediately below and above sea level (205/59, 205/38). The Kieler Ufer Section also contains a duplex stack in its central part. The individual elements are KU3d3, KU3d2, and KU3d1. All of these sheets represent S-type segments, according to the duplex-stack model. The individual thrust sheets KU4 in the south as well as KU2 and KU1 in the north surround this duplex stack (Figs. 4c and 5a). Their frontal ramps dip towards the SSW or SW (Table 1). The distal zone of the southern JGC comprises both the Kollicker Bach and Stubbenkammer Section. The Kollicker Bach Section simply shows an imbricate fan with three thrust sheets KB3, KB4, and KB1, while the Stubbenkammer Section shows an imbricate thrust system with three individual thrust sheets SK3, SK2, and SK1 in the north and a duplex stack in the south containing SK4d3, SK4d2, and SK4d1. The lower and middle duplex segments SK4d1 and SK4d2 show an S-type shape, while the upper segment SK4d3 has been determined to be a G( $\Gamma$ )-type element. The thrust faults of the Kollicker Bach and Stubbenkammer Section are inclined towards S/SSW – e.g. the frontal ramp of SK2 with 185/57 and KB2 with 210/50 (Table 1).

All in all, structures indicative of intense deformation to form duplex stacks are included in the Tipper Ort Section and Kieler Ufer Section that make up part of the central zone, and in the Stubbenkammer Section of the distal and northernmost part of the southern JGC. The highest elevations of the modelled southern JGC are represented by the hanging-wall anticlines of the central zone (166 m a. s. l.), which confirms the intense deformation and horizontal shortening represented in this instance by several duplex stacks (Table 1, Figs. 3, 4, 5). The most proximal Gakower Ufer Section and the most distal Stubbenkammer Section also show high elevations (145 m, 147 m). The length of the thrust sheets ranges from about 200 to 550 m (Table 1). The longest sheets are located in the Schnaks Ufer Section (SU3 and SU1: 699 m, 745 m) and Kieler Ufer Section (lowermost duplex segment KU3d1: 820 m). The thickness of the beds ranges from about 100 to 150 m (Table 1).

In general, the thrust faults are moderately to steeply inclined throughout the entire cliff section of the southern JGC. In the best-fit model, they often splay from the décollement with a gentle inclination and turn into steeper faults at hinge points located below the cliff base (Figs. 3, 4, 5, Table 1). The steepest thrust faults can be found in the proximal Gakower Ufer Section (e.g. 220/81). The southern JGC contains three reverse faults (“S09a”, KU4, and SK4d3), which can be safely interpreted as pre-Quaternary faults as they do not disrupt the Pleistocene beds. The other faults are presumably branching fault segments, which are here referred to as satellite faults. These faults are younger and associated with glacitectonism in the southern JGC.

## The restored cross sections and their kinematic information

The entire restored cross section of the southern JGC represents the bedding conditions and tectonic state prior to the glacitectonic deformation (Figs. 3d, 4c, 5a, b). The model shows a simplified bedding, which still indicates some thickness variation and offset. The reverse faults in the thrust sheets “S09a”, KU4, and SK4d3, as well as the tectonic offsets between certain thrust sheets, detected in the restored cross section may indicate pre-glacitectonic deformation characterised by faulting. In general, the restored sections show the top of the Cretaceous chalk unit at or close to the beach level. The escarpment between the Gakower and Wissower Ufer Section (GU1/WU3) seems to be related to the changing depth of the décollement zone, which might be the position of the pre-existing décollement of the northern JGC. The restored cross section of the Kollicker Bach Section shows distinct escarpments between all thrust sheets. They appear to indicate reverse faults inclined towards the southwest with vertical offsets of ca. 14 and 31 m. The offsets can be confirmed by the topmost flint layer as represented by F54 in each thrust sheet (Tab. 1).

Throughout the entire restored cross section of the southern JGC, the stratigraphy at the top of the chalk unit with the flint layers F54 to F56 is relatively uniform (Tab. 1). The topmost chalk succession of the Gakower Ufer Section in the most proximal zone is distinctly older, probably F50 to F53 or F38 and F46 according to Steinich (1972). Thickness differences between flint layers in adjacent thrust sheets (see also Wissower Ufer, Tipper Ort) can be an effect of primary bed-thickness variations or also of volume loss, which can occur during the glacitectonic deformation.

The Pleistocene deposits have constant thicknesses around 10–15 m. However, in certain (footwall) synclines they can be very thick, especially in the trailing edge of TO1 with 63 m or KB1 with 31 m (Figs. 4c and 5a). The significant increase in the thickness of footwall synclines may be due to piggyback basins (in the sense of Pedersen 2005). The thickness of the Pleistocene unit in GU4 and GU3 is assumed to be overestimated in this best-fit model as it is an effect of the thick Pleistocene succession in the syncline of S01a (Fig. 3c). The original thickness is assumed to have been not that high in the Gakower Ufer Section and was probably similar to GU2 and GU1.

The modelled cross sections reveal a local glacier push from S/SW to N/NE, when the southern JGC was formed. This is confirmed by the structural data of the ramps, which are summarised in Table 1. The tectonic transport in the Gakower Ufer Section may have been directed from SW to NE, as the ramps generally dip towards the SW (Table 1). In the Wissower Ufer Section, the local tectonic transport may have changed to a direction from WSW to ENE. The

transport in the Schnaks Ufer Section seems to have been directed from the SW/WSW to NE/ENE. The thrust faults of the northwards following sections (Tipper Ort, Kieler Ufer, Stubbenkammer) dipping to S/SSW indicates transport directed from S/SSW to N/NNE. An exception is the Kollicker Bach Section where ramps are inclined towards the SW.

Some of the cross sections are not perfectly balanced due to missing data (Figs. 3d, 4c, 5a, b). There are gaps in the frontal ends of the restored thrust sheets. The largest gaps appear in GU4 in the Gakower Ufer Section, as well as in WU2 and WU1 of the Wissower Ufer Section. Other large gaps occur in the northern ends of the restored thrust sheets of TO1, TO2d1, and TO3 of the Tipper Ort Section as well as KU3d2 in the Kieler Ufer Section. The Kollicker Bach Section shows such obvious gaps, for example, in the frontal ends of KB3 and KB2, the Stubbenkammer Section in SK4d1, SK3, and SK2. These larger gaps indicate a fair quantity (up to ca. 30% of a single thrust sheet) of missing bed lengths in certain parts of the restored cross sections.

### Horizontal shortening

The minimum horizontal shortening of the southern JGC was determined to be 5510 m (49.1%). Thus, the original pre-glacitectonic cross section was 11,230 m long, compared to its present deformed length of ca. 5720 m, when considering the average azimuths of the modelled cross sections. A summary of the horizontal shortening in each section and thrust sheet is given in Table 2.

In consideration of the horizontal shortening of the southern JGC, the minimum shortening of the Gakower Ufer and Wissower Ufer Section was less than 40%, respectively. The Gakower Ufer Section shows a horizontal shortening of 675 m (37.4%). The initial length of the Wissower Ufer Section is calculated to at least 1050 m. It has been shortened by a minimum of 417 m (39.7%).

The central zone of the southern JGC is characterised by more extensive shortening. This is already obvious in the Schnaks Ufer Section with an initial length of at least 1872 m and a present length of 944 m, which reveals a horizontal shortening of at least 928 m (49.6%). The duplex stacks observed in the Tipper Ort and Kieler Ufer Section show the highest amount of horizontal shortening in the southern JGC. The Tipper Bach Section shows a local horizontal shortening of at least 916 m (51.2%). The Kieler Ufer Section has been shortened by minimum 1280 m (51.6%). Additionally, the quasi-parallel composite ridges of the southern JGC (Fig. 1c) show certain bifurcations, which lead to an increase of the number of ridges especially towards the central area implying increased deformation in this zone.

The most distal zone is less strongly deformed than the central part. The initial length of the Kollicker Bach Section

has been determined to at least 1320 m. Now, the section measures 920 m. Thus, the entire horizontal shortening of the Kollicker Bach Section is minimum 400 m (30.3%). Although the Stubbenkammer Section in this distal part shows a less complicated structural configuration than the central zone, it was still strongly shortened, which led to the horizontal shortening of 49.8% (minimum 1142 m).

### Partitioning of deformation mechanisms

The most proximal part of the southern JGC is fold-thrust-dominated. However, the structures turn into imbricate stacks subjected to fault-bend folding only after at least 800 m towards the north. Thus, faulting is still dominant with about 65.5% of the total shortening in the Gakower and Wissower Ufer sections accommodated by this mechanism, even though the proximal zone indicates more folding (GU2, GU1, WU3) than the central and distal part of the southern JGC. The amounts of folding as well as the consolidation and translation for each section and thrust sheet are given in Table 2. When the proximal zone transitions into the central zone (Schnaks Ufer Section), the process of folding constitutes only 15.8% (147 m) of the entire deformation. The translation component also presents a minimum value of 84.2% (781 m). The central zone of the southern JGC is more thrust-dominated. Translation along the décollement surface, ramps, intermediate and upper flats is considered to represent the dominant part of shortening. The northern part of the southern JGC is also thrust-dominated. The results of deformation partitioning indicate that faulting (81.9% of the total shortening) was the main form of deformation in the northernmost zone (Stubbenkammer Section). The Kollicker Bach Section does not show such a high amount of shortening (30.3%), compared to the sections of the central zone and the distal Stubbenkammer Section. However, the structural configuration might be more complicated than shown in the best-fit model presented here.

### Interpretation and discussion

#### Kinematic model of progressive ice-marginal deformation for the Jasmund Glacitectonic Complex

According to the models based on the morphology, sedimentology, and age determination of the JGC (e.g. Gehrmann and Harding 2018; Plonka et al. 2021; Kenzler et al. 2022), the structural development of the entire complex took place in the late Weichselian and is characterised by a polyphase evolution. The main formation of the southern part occurred in the second evolutionary phase, when the second glaci-tectonically effective glacier lobe of the Scandinavian Ice Sheet locally moved from SE to NW (see Fig. 1c, Gehrmann

**Table 2** Summary of the shortening and portions of deformation mechanisms (folding, faulting) in the individual sections

Sections	Total minimum shortening		Folding part		Translation and consolidation part (mm)		Fraction of total shortening (%)	Thrust sheets	Shortening (folding) (m)	Displacement along individual thrust fault (m)
	Absolute value (m)	Percentage (%)	Absolute value (m)	Fraction of total shortening (%)	Absolute value (m)	Absolute value (m)				
Gakower Ufer section	675	37.4	> 233	> 34.5	442	65.5	S01a	GU4	53	209
							S01b	GU3	34	36
							S02	GU2	98	202
Wissower Ufer section	417	39.7	142	34.1	275	65.9	S03	GU1	48	174
							S04a	WU3	59	125
							S04b	WU2	41	196
							S04c	WU1	42	217
Schnaks Ufer section	928	49.6	147	15.8	781	84.2	S05	SU3	45	211
							S06	SU2	72	294
							S07	SU1	30	475
Tipper Ort section	916	51.2	325	35.5	591	64.5	S08	TO3	84	167
							S09c	TO2d2	182	358
							S09b	TO2d1	31	358
							S10	TO1	28	182
Kieler Ufer section	1280	51.6	263	20.5	1017	79.5	S11	KU4	34	243
							S12	KU3d3	46	438
							S13	KU3d2	26	521
							S14	KU3d1	80	328
Kollicker Bach section	400	30.3	151	37.7	249	62.3	S15	KU2	17	164
							S16	KU1	60	206
							S17	KB3	63	199
							S18	KB2	32	194
Stubbenkammer section	1142	49.8	207	18.1	935	81.9	S19	KB1	56	252
							S20-1	SK4d2/SK4d3	59	379
							S20-2	SK4d1	20	215
							S21	SK3	51	79
							S22	SK2	28	262
							S23	SK1	49	–

The absolute shortening values of folding and the displacement along the individual thrust faults of each thrust sheet are given in addition. The shortening results of the individual thrust sheets do not include the translation along the décollement and satellite faults

and Harding 2018). This development model is supported and advanced further by the results of the structural analysis presented here.

Considering the dip direction of most of the thrust faults falls towards S or SW, together with the composite ridges of the southern JGC with SW-NE orientation exhibiting a concave shape towards the SE as visible in the DEM (see Fig. 1c), a piedmont-type lobe is suggested for the advancing glacier front, which pushed generally from the SE to NW. This resulted in a local S to N or even SW to NE push at the area of today's east coast. Figure 6 shows a simplified summary of all structures in the southern JGC, which developed sequentially during proglacial deformation (Stages A to E). In general, the tectonic evolution of the southern JGC contains three mechanisms of shortening, similar to the analogue model suggested by Dixon and Liu (1992) with layer-parallel shortening, folding, and thrusting.

In *Stage A*, the northern JGC has already formed and is supposed to exist at the position shown in Fig. 6 with a décollement zone at presumably 120 m below today's sea level. When the lobe of the SIS reached the Prorer Wiek area southeast of Jasmund (Fig. 1c) in *Stage B*, it is suggested that layer-parallel shortening occurred in the form of consolidation of the upper ca. 90 m of the ice-marginal and proglacial deposits. When the failure limit of the deposits was exceeded, buckle folds nucleated along a décollement zone from the hinterland to the foreland. The buckles can be regarded as detachment folds.

The progressive glacier advance led to intensified contraction in the 90 m-thick consolidated and folded layer during *Stage C*. When the capacity of the deposits to deform as an elastic body was exceeded, fractures were initiated. These fractures developed into ramps in the distal limb of the anticlines, with initial angles between 30° and 45°. The progressive folding indicates a transition from detachment folds into fault-propagation folds in front of the glacier, while new detachment folds were formed towards the foreland. The sequential formation of multiple anticline-syncline pairs in a primary deformation phase and thrusting in a secondary phase was also presented for the modern Eyjabakkajökull end moraine in Iceland (Benediktsson et al. 2010).

With progressive deformation in the southern JGC during *Stage D*, folding was increasingly followed by thrusting as the deformation could no longer be compensated by plastic behaviour. Possible influencing factors might be the decrease of space due to the northern JGC acting as a buttress or the presence of frozen ground, changes in the deformation velocity, high porewater pressures as well as rheological reasons such as variations in the shear strength of the chalk. Moreover, fault-propagation folding transitioned into fault-bend folding by breakthrough thrusting (see Mitra 1990; Mercier et al. 1997; Brandes and Tanner 2014). While folds were still forming in the distal part representing less mature

structures, the structures in the proximal and central zone of the complex were strongly superimposed by the formation of new ramps towards the foreland. Already existing gently dipping thrust faults were passively tilted and even oversteepened. The décollement surface likely shifted from 90 m through 105 m down to 120 m below the today's beach level. The Gakower Ufer Section in the proximal zone with its SW-vergent folds, high elevations, and steep thrusts indicates a strong deformation and modification of structures occurred close to the advancing glacier front. The section emphasizes the occurrence of a high-strain zone located between the advancing glacier from the south and the northern JGC that acted as a buttress.

During *Stage E*, fold and thrust-fault propagation ceased to migrate in the distal zone. Moreover, already existing faults of the northern JGC were intensively superimposed by the ice moving towards the NW (locally N/NE in the zone of the today's cliff). Even the deformation in the fault-bend folds could not be compensated by folding in this high-strain area. The progressive glacier push and deformation facilitated the development of satellite faults in the hanging-wall anticlines. They formed as reverse faults nucleating from the frontal ramp when the capacity of the chalk strata to deform as an elastic body was exceeded in the hanging-wall anticlines. These satellite faults represent the youngest faults, which have been restored first in the cross-section restoration. In addition, duplex stacks may have formed during this stage indicating large-magnitude shortening.

When the central and distal parts of the southern JGC formed, piggyback basins may have developed in the thrust sections TO2d1, TO1, KB1, and SK1. The potential evolution of piggyback basins in these districts would imply that the thrust sheets TO2d1, TO1, KB1, and SK1 might have been translated along the flat over a longer period of time. The other thrust sheets, particularly those of the proximal zone, seem to have imbricated at a faster rate, since the potential basins were trapped by overthrusting of the hanging-wall block. Such syntectonic deposition in a piggyback manner was described by Plonka et al. (2021) for the outcrop Dwasieden southwest of Sassnitz and Gibb (2015) for the section "S25" in the northern JGC. However, detailed structural and sedimentological investigations of these basins in the Tipper Ort, Kollicker Bach, and Stubbenkammer Section are needed to verify the existence of piggyback basins in the southern JGC.

After the formation of the northern and southern JGC by two different glacier lobes of the SIS (evolutionary stages 1 and 2 in Gehrman and Harding 2018), a re-advance of the Scandinavian Ice Sheet occurred (Pomeranian/Mecklenburg—W2/W3). The ice sheet is assumed to have overridden the entire JGC or at least the marginal parts. This led to massive erosion of the glacitectonised sequence and subsequent deposition of the M3-till complex (see, e.g. Fig. 4b).

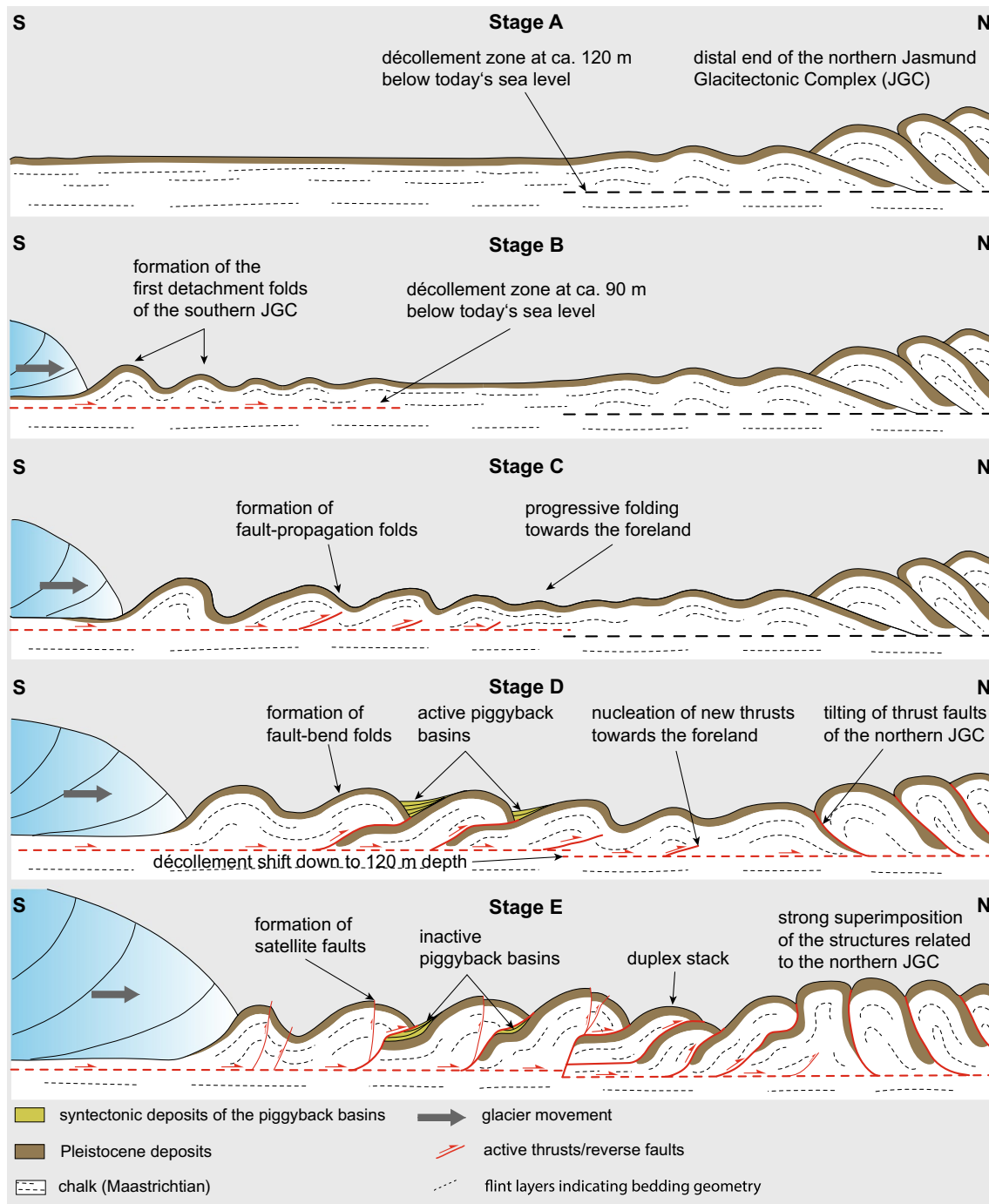


**Fig. 6** Simplified model of progressive deformation for the southern Jasmund Glacitectonic Complex (JGC) in the second evolutionary phase (general glacier movement from SE to NW) of the multi-phase model suggested by Gehrmann and Harding (2018) (see Fig. 1c). The development is illustrated in a sequence of glacitectonic stages indicating the progressive proglacial deformation. Stage A: Situation after the formation of the northern JGC and prior to the formation of the southern JGC; Stage B: Detachment folding in front of the advancing glacier; Stage C: Transition into fault-propagation fold-

ing by continuation of glacier advance; Stage D: Fault-bend folding, nucleation of new folds and thrusts towards the foreland, tilting of thrust faults in the northern JGC; Stage E: development of more complex structures like satellite faults and duplex stacks due to progressive deformation by continued glacier advance, superimposition of the structures in the northern JGC. The model is not true to scale and reduced to a few thrust sheets indicating the most prominent structures, which developed by the glacitectonic folding and thrusting

An exact assignment of the uppermost deposits to the glaciations of the Pomeranian and Mecklenburg stage was not attempted, as there is not enough data so far to fully assign all processes to the major phases.

### Line length vs. flexural slip balancing

The application of restoration techniques in modern software leads to an enormous time saving and provides the opportunity to check different geometries and algorithms. However, the different assumptions and methods used by the software need to be explored to produce the geologically most realistic cross sections. Thus, various steps of kinematic restoration and different algorithms—especially Line Length vs. Flexural Slip, were tested in this study.

The restored cross sections still produced smaller residual folds after applying the Flexural Slip algorithm, which could be manually adjusted afterwards (Fig. 7a). The results indicate certain bedding characteristics of each section, as the process maintains thickness variations. This cannot be detected using the Line Length algorithm. However, Line Length quickly led to the required straight beds in the

restored cross section (Fig. 7b). Thus, Line Length was preferred as the main algorithm in the restoration workflow, as it easily facilitated horizontal shortening calculations. In most cases, the modelling workflow was stopped immediately after the Flexural Slip application to obtain information about certain bedding characteristics such as tectonic or non-tectonic volume changes. Then, the workflow was restarted using the Line Length function.

### The glacitectonic deformation model in the context of fold-and-thrust belts, its issues and potential

Modern glacitectonic complexes are known for instance from the glacier forefields of Eyjabakkajökull and Brúarjökull in Iceland (e.g. Ingolfsson et al. 2016) or Holmströmbreen on Svalbard (e.g. Gripp 1929; Boulton et al. 1999). The deformation structures originating from ice-marginal or proglacial deformation are similar to those of large-scale fold-and-thrust belts in terms of geometry and formation processes. Similar to the orogenic thin-skinned thrust tectonics, glacitectonic complexes can be organised into flat and ramp architecture. When the ramps emerge, they usually dip

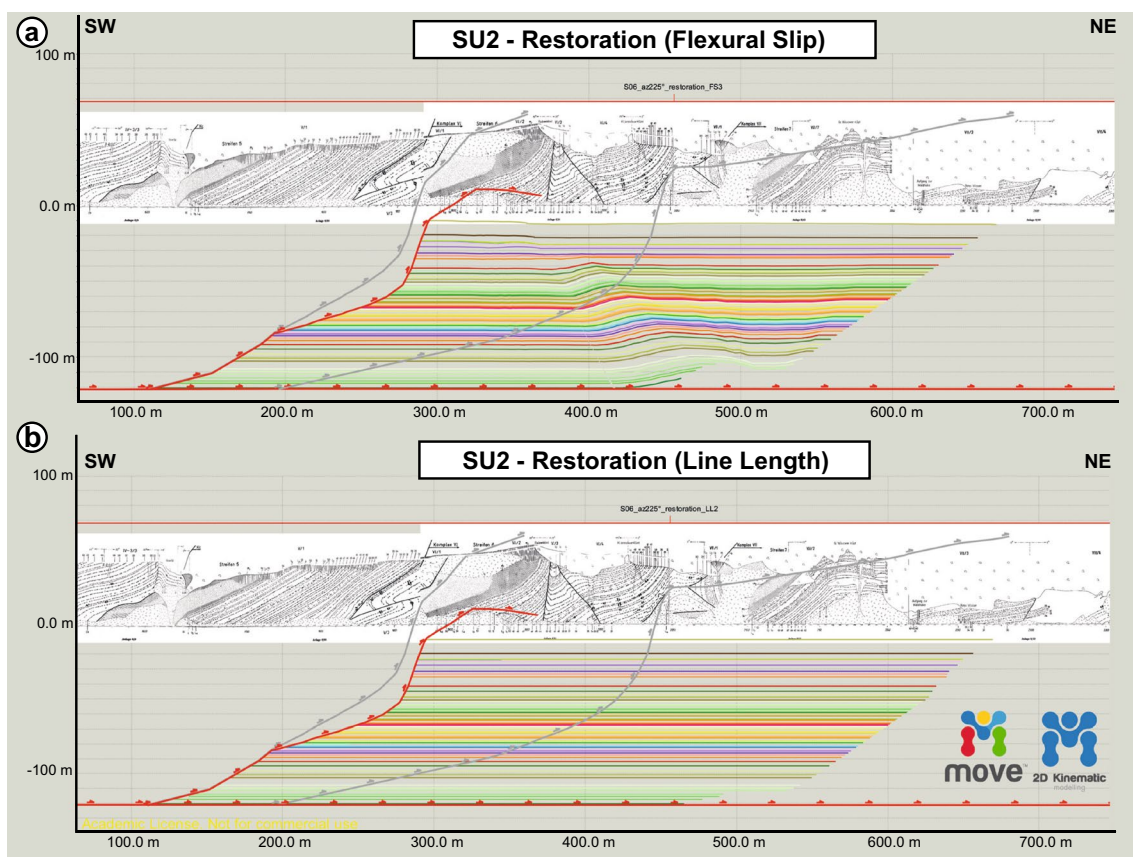


**Fig. 7** Contrasting juxtaposition of the exemplary restored thrust sheet SU2 (Schnaks Ufer Section) resulting from the two different algorithms. **a** Restoration result from the application of the Flexural

Slip algorithm. **b** Restoration result from the application of the Line Length algorithm. The original cross sections constructed by Steinich (1972), are shown in the background

at angles of less than 30°. New thrusts form towards the foreland, which leads to progressively flatter and younger thrusts in the direction of tectonic transport (e.g. Boyer and Elliott 1982; Pedersen 2005). However, glacitectonic fold-thrust complexes differ from orogenic fold-and-thrust belts primarily in scale, deformation rate, and shallowness of penetrative deformation (Pedersen 2005).

In such glacial landforms known as composite ridges, the deformation can extend to a depth of a few tens of metres and down to 200 m (Aber et al. 1989; van der Wateren 2003; Phillips 2018). The JGC with its décollement zone at 90–120 m below today's beach level, is an example of large composite ridges or glacitectonic complexes similar to documented onshore complexes (e.g. Pedersen 2000; Bennett 2001) and offshore (e.g. Pedersen and Boldreel 2017; Lohrberg et al. 2021). In such complexes, thrust faults dip towards the proximal zone of the complex and towards the proposed ice margin (Vaughan-Hirsch and Phillips 2017). This geometry is consistent with our findings from the structural analysis of the southern JGC and the comparison with the associated morphology (see Fig. 1c).

Resolving the details of fold-thrust structures exposed in the northern JGC remains the main challenge addressed by the refined model presented in this paper. The northern JGC acted as a buttress in the north of the southern JGC (see Fig. 6), where it stopped further fold and thrust-fault propagation in the distal zone of the southern JGC, which at some point lead to massive shortening and complicated deformation. Thus, the strain decrease from the central zone towards the foreland, which can be observed in all classic glacitectonic complexes is not typical of the southern JGC. The observed geometry of the décollement in the JGC with a climb from lower elevations in the proximal zone (ca. 90 m b. s. l.) to deeper elevations in the distal zone (ca. 120 m b. s. l.) is also not characteristic of classic glacitectonic complexes. This might be related to the existence of a pre-existing décollement zone in the northern JGC.

In the progressive deformation model, a quasi-horizontal palaeo-surface was assumed for the beginning of the southern JGC formation (see Fig. 6). Considering well logs from the area outside the JGC, the present boundary between the Cretaceous and Pleistocene unit lies at around 40 m b. s. l. (see Hoth et al. 1993). Since the thickness of the older Pleistocene deposits (M1 to I2) is between ca. 10 m and 40 m (adopted from field data and modelled cross sections), the palaeo-surface is assumed to have been nearly at the same position as today's sea level. This, however, is a crude assumption. As there were several pre-Quaternary faults with offsets of up to 5 m, the surface may have had at least small escarpments.

The model proposed here demonstrates the relationship between the southern and northern JGC, which is characterised by several glacitectonic phases and superimposed

deformations. It is clear from the large gaps at the frontal ends of several of the restored thrust sheets that a 2D interpretation and a plane strain model are probably too simple assumptions for the tectonic setting of Jasmund. Tectonic erosion is the most plausible explanation for gaps with larger volume loss in the upper thrust-sheet parts, as the upper beds were subjected more to transport along the ramps than the lower beds. When bed lengths are lacking in the lower frontal parts of the thrust sheets or when these gaps are too large, they imply errors of the modelled 2D fault geometry at depth leading to unbalanced cross sections. However, there are some random dip directions of thrust faults recognizable in the field and corresponding to the modelled cross sections, which do not fit into the general model of a local glacier push from southeast to northwest. Furthermore, the glacial geomorphology demonstrated in the DEM (Fig. 1c) and discussed by Gehrmann and Harding (2018) confirms a polyphase deformation of the entire glacitectonic complex. Thus, we suggest a complex 3D deformation model, which involves the superimposed-deformation approach suggested by Pedersen (2000) for glacitectonic complexes.

The structural analysis of Jasmund and the comparison with ancient and modern glacitectonic complexes indicate a spatial and temporal development of fault-related folding in a fold-and-thrust belt. Cross-section restoration of the southern JGC, together with the calculation of horizontal shortening, enabled quantification of strain associated with ice-marginal glacitectonism at this part of the southern SIS margin. The investigation presented here clearly shows how structural modelling software such as Move and associated tools can be applied to glacitectonic complexes. We provided a structural contribution to strengthen the geomorphological model presented by Gehrmann and Harding (2018) and confirm that the southern JGC formed in a second evolutionary stage during a local glacier push from a southern direction. However, the structure of Jasmund is more complicated and we suggest superimposed deformation played an important part in the evolution of the JGC. Our results indicate similarities and important differences between the JGC and other Pleistocene and modern glacitectonic complexes, but also a detailed study highlighting the intricate and individual architecture of Jasmund. It provides new insight into the deformation and shortening history of this spectacular complex of the southwestern Baltic Sea coastline.

## Conclusions

- The southern JGC represents a fold-and-thrust belt, more precisely a glacitectonic imbricate thrust system. The décollement zone is situated at ca. 90 m and 105 m b. s. l. in the most proximal zone, but 120 m b. s. l. in the main part. Several syncline–anticline pairs represent the struc-



tural inventory in the proximal zone of the southern JGC. The central and distal zones indicate a complicated imbricate fan with different duplex stacks. Satellite faults are frequent in hanging-wall anticlines.

- The suggested kinematic model provides extended and detailed information about the geomorphological model by Gehrman and Harding (2018). After the formation of the northern JGC, a particular piedmont-type lobe of the southern Scandinavian Ice Sheet margin locally moved from SE to NW. Structural analysis and matching of the balanced cross sections with geomorphological information revealed that a local glacier push led to the formation of thrust faults mainly dipping towards the S/SW.
- The structural evolution of the southern JGC is characterised by a temporal continuum of fault-related folds, which develop from detachment folds over fault-propagation folds to fault-bend folds.
- The entire horizontal shortening of the southern JGC is 5510 m (49.1%). Partitioning of deformation mechanisms into folding and faulting portions reveal that the displacement along the décollement and thrust faults dominated throughout the entire section compared to folding. However, the amount of folding was higher in the most proximal zone than in the central and distal zones. According to the definitions given by Boulton et al. (1999), the most proximal southern part of the southern JGC is fold-thrust-dominated turning into thrust-dominated parts towards north.
- The southern JGC deviates from classic glaciectonic complexes by a number of structural anomalies, like massive deformation and horizontal shortening in the distal zone and an anomalous shift of the décollement down to deeper positions. Furthermore, the restored cross section shows gaps at the frontal end of certain thrust sheets. These results may reflect superimposed deformation in the glaciectonic complex.

**Acknowledgements** We thank Midland Valley Exploration Ltd. and Petex for providing the software Move™. Additionally, we thank the Nationalparkamt Vorpommern and Dr. Ingolf Stodian (Nationalpark Jasmund) for the good collaboration and for the approval to work in the national park. The LiDAR data of Jasmund were provided by the Landesamt für innere Verwaltung – Abt. für Geoinformation, Vermessung und Katasterwesen. Jörg Hartleib (Institute of Geography and Geology, University of Greifswald) processed the data. We thank Laurence Warr for English proof-reading. In addition, we thank Ulrich Riller and the reviewers David Tanner and Bernhard Grasemann for the positive and inspiring reviews. This research did not receive any specific grant from funding agencies in the public, commercial, or not-for-profit sectors.

**Funding** Open Access funding enabled and organized by Projekt DEAL.

## Declarations

**Conflict of interest** The authors declare that they have no known competing financial interests or personal relationships that could have appeared to influence the work reported in this paper.

**Open Access** This article is licensed under a Creative Commons Attribution 4.0 International License, which permits use, sharing, adaptation, distribution and reproduction in any medium or format, as long as you give appropriate credit to the original author(s) and the source, provide a link to the Creative Commons licence, and indicate if changes were made. The images or other third party material in this article are included in the article's Creative Commons licence, unless indicated otherwise in a credit line to the material. If material is not included in the article's Creative Commons licence and your intended use is not permitted by statutory regulation or exceeds the permitted use, you will need to obtain permission directly from the copyright holder. To view a copy of this licence, visit <http://creativecommons.org/licenses/by/4.0/>.

## References

- Aber JS, Croot DG, Fenton MM (1989) Glaciectonic landforms and structures. Kluwer, Dordrecht
- Benediktsson ÍÖ, Schomacker A, Lokrantz H, Ingólfsson Ó (2010) The 1890 surge end moraine at Eyjabakkajökull, Iceland: a re-assessment of a classic glaciectonic locality. *Quat Sci Rev* 29:484–506. <https://doi.org/10.1016/j.quascirev.2009.10.004>
- Bennett MR (2001) The morphology, structural evolution and significance of push moraines. *Earth Sci Rev* 53:197–236. [https://doi.org/10.1016/S0012-8252\(00\)00039-8](https://doi.org/10.1016/S0012-8252(00)00039-8)
- Berthelsen A (1978) The methodology of kineto-stratigraphy as applied to glacial geology. *Bull Geol Soc Den* 27:25–38
- Boulton GS, van der Meer JJM, Beets DJ, Hart JK, Ruegg GHJ (1999) The sedimentary and structural evolution of a recent push moraine complex: Holmströmbreen, Spitsbergen. *Quatern Sci Rev* 18:339–371. [https://doi.org/10.1016/S1571-0866\(04\)80103-9](https://doi.org/10.1016/S1571-0866(04)80103-9)
- Boyer SE, Elliott D (1982) Thrust systems. *Am Asso Petrol Geol Bull* 66:1196–1230
- Brandes C, Tanner DC (2014) Fault-related folding: a review of kinematic models and their application. *Earth Sci Rev* 138:352–370. <https://doi.org/10.1016/j.earscirev.2014.06.008>
- Credner R (1893) Rügen. Eine Inselstudie. *Forschungen Zur Deutschen Landes- Und Volkskunde* 7:373–494
- Croot DG (1987) Glacio-tectonic structures: a mesoscale model of thin-skinned thrust sheets? *J Struct Geol* 9:797–808. [https://doi.org/10.1016/0191-8141\(87\)90081-2](https://doi.org/10.1016/0191-8141(87)90081-2)
- Croot DG (1988) Morphological, structural and mechanical analysis of neoglaciac ice-pushed ridges in Iceland. In: Croot DG (ed) *Glaciectonics: forms and processes*. Balkema, Rotterdam, pp 33–47
- Dahlstrom CDA (1969) Balanced cross sections. *Can J Earth Sci* 6:743–757. <https://doi.org/10.1139/e69-069>
- Dixon JM, Liu S (1992) Centrifuge modelling of the propagation of thrust faults. In: McClay KR (ed) *Thrust tectonics*. Chapman and Hall, London, pp 53–70
- Egan SS, Buddin TS, Kane SJ, Williams GD (1997) Three-dimensional modelling and visualisation in structural geology: new techniques for the restoration and balancing of volumes. In: *Proceedings of the 1996 Geoscience Information Group Conference on Geological Visualisation, Electronic Geology* 1(7):67–82
- Gehrman A, Harding C (2018) Geomorphological mapping and spatial analyses of an upper weichselian glaciectonic complex based

- on LiDAR Data, Jasmund Peninsula (NE Rügen) Germany. *Geosci* 8(6):208. <https://doi.org/10.3390/geosciences8060208>
- Gehrmann A, Hüneke H, Meschede M, Phillips ER (2017) 3D microstructural architecture of deformed glacial sediments associated with large-scale glaciectonism, Jasmund Peninsula (NE Rügen) Germany. *J Quat Sci* 32(2):213–230. <https://doi.org/10.1002/jqs.2843>
- Gehrmann A, Meschede M, Hüneke H, Pedersen SAS (2019) Sea cliff at Kieler Ufer (Pleistocene stripes 11–16)—large-scale architecture and kinematics of the Jasmund Glacitectonic Complex. *DEUQUA Spec Publ* 2:19–27. <https://doi.org/10.5194/deuquasp-2-19-2019>
- Gibb A (2015) Sedimentarchitektur und Fazies der interstadialen Sedimente am Stubbenhörn—Abbild glazitektonischer Prozesse (Jasmund, Rügen). Bachelor thesis, University of Greifswald
- Gripp K (1929) Glaziologische und geologische Ergebnisse der Hamburgischen Spitzbergen-Expedition. *Abhandlungen Des Naturwissenschaftlichen Vereins Hamburg* 22:147–247
- Gripp K (1947) Jasmund und Möen, eine glacialmorphologische Untersuchung. *Zeitschrift Zur Erdkunde* 1:175–182
- Groth K (2003) Zur glazitektonischen Entwicklung der Stauchmoräne Jasmund/Rügen Schriftenreihe Des Landesamtes Für Umwelt, Naturschutz Und Geologie Mecklenburg-Vorpommern 3:39–49
- Hoth K, Rusbült J, Zagora K, Beer H, Hartmann O (1993) Die tiefen Bohrungen im Zentralabschnitt der mitteleuropäischen Senke—Dokumentation für den Zeitabschnitt 1962–1990. Schriftenreihe für Geowissenschaften 2
- Houmark-Nielsen M (1987) Pleistocene stratigraphy and glacial history of the central part of Denmark. *Bull Geol Soc Denmark*. <https://doi.org/10.37570/bgsg-1988-36-01>
- Houmark-Nielsen M (2007) Extent and age of Middle and Late Pleistocene glaciations and periglacial episodes in Southern Jylland, Denmark. *Bull Geol Soc Denmark* 55:9–35. <https://doi.org/10.37570/bgsg-2007-55-02>
- Inglósson Ó, Benediktsson ÍÓ, Schomacker A, Kjær KH, Brynjólfsson S, Jónsson SA, Korsgaard NJ, Johnson MD (2016) Glacial geological studies of surge-type glaciers in Iceland—research status and future challenges. *Earth Sci Rev* 152:37–69. <https://doi.org/10.1016/j.earscirev.2015.11.008>
- Jaekel O (1917) Neue Beiträge zur Tektonik des Rügener Steilufers. *Zeitschrift Der Deutschen Geologischen Gesellschaft* 69:81–176
- Janke W, Niedermeyer R-O (2011) Geologische Entwicklung im Pleistozän. In: Niedermeyer R-O, Lampe R, Janke W, Schwarzer K, Duphorn K, Kliewe H, Werner F (eds) *Die deutsche Ostseeküste*. Gebr. Borntraeger Verlagbuchhandlung, Stuttgart, pp 32–51
- Johnstrup F (1874) Ueber die Lagerungsverhältnisse und die Hebungssphänomene in den Kreidefelsen auf Möen und Rügen. *Zeitschrift Der Deutschen Geologischen Gesellschaft* 26:533–585
- Kane SJ, Williams GD, Buddin TS, Egan SS, Hodgetts D (1997) Flexural-slip based restoration in 3D, a new approach. In: AAPG Annual Convention Official Program. A58
- Katzung G, Müller U (2004) Quartär. In: Katzung G (ed) *Geologie von Mecklenburg–Vorpommern*. E. Schweizerbart'sche Verlagsbuchhandlung, Stuttgart, pp 221–225
- Keilhack K (1912) Die Lagerungsverhältnisse des Diluviums in der Steilküste von Jasmund auf Rügen. *Jahrbuch Der Preußischen Geologischen Landesanstalt* 33:114–158
- Kenzler M, Obst K, Hüneke H, Schütze K (2010) Glazitektonische Deformation der kretazischen und pleistozänen Sedimente an der Steilküste von Jasmund nördlich des Königsstuhls (Rügen). *Brandenburgische Geowissenschaftliche Beiträge* 17:107–122
- Kenzler M, Krauß N, Hüneke H (2022) Testing a proposed new chronology for the Jasmund Glacitectonic Complex (SW Baltic Sea): no indication of incipient deformation during MIS 3. *Quat Geochronol* 70:101299. <https://doi.org/10.1016/j.quageo.2022.101299>
- Litt T, Behre K-E, Meyer K-D (2007) Stratigraphische Begriffe für das Quartär des norddeutschen Vereisungsgebietes. *E&G Quat Sci J* 56:7–65. <https://doi.org/10.23689/figeo-1278>
- Lohrberg A, Krastel S, Unverricht D, Schwarzer K (2021) The Heliogoland Glacitectonic Complex in the southeastern North Sea: indicators of a pre- or early-Elsterian ice margin. *Boreas*. <https://doi.org/10.1111/bor.12551>
- Ludwig AO (1954/55) Eistektonik und echte Tektonik in Ost-Rügen (Jasmund). *Wissenschaftliche Zeitschrift der Ernst-Moritz-Armdt-Universität Greifswald, Mathematisch-naturwissenschaftliche Reihe* 4(3/4):251–288
- Ludwig AO (2005) Zur Interpretation des Kliffanschnitts östlich Glowe/Insel Rügen (Ostsee). *Z Geol Wiss* 33:263–272
- Ludwig AO (2006) Cyprinenton und I1-Folge im Pleistozän von Nordost-Rügen und der Insel Hiddensee (südwestliche Ostsee). *Z Geol Wiss* 34:349–377
- Ludwig AO (2011) Zwei markante Stauchmoränen: Peski/Belorusland und Jasmund, Ostseeinsel Rügen/Nordostdeutschland – Gemeinsame Merkmale und Unterschiede. *E&G Quat Sci J* 60(4):464–487. <https://doi.org/10.23689/figeo-1757>
- Mehlhorn P, Winkler L, Grabbe F-C, Kenzler M, Gehrmann A, Hüneke H, Rother H (2019) Coastal cliff at Lenzer Bach on Jasmund Peninsula, Rügen Island (Pleistocene Stripe 4): reconstructed history of glaciectonic deformation based on fold geometry and microstructural mapping. *DEUQUA Spec Publ* 2:35–41. <https://doi.org/10.5194/deuquasp-2-35-2019>
- Mercier E, Outtani F, Frizon de LaMotte D (1997) Late-stage evolution of fault-propagation folds: principles and examples. *J Struct Geol* 19:185–193. [https://doi.org/10.1016/S0191-8141\(96\)00081-8](https://doi.org/10.1016/S0191-8141(96)00081-8)
- Midland Valley Exploration Ltd (2017) Move2017.1 suite, Glasgow
- Mitra S (1990) Fault-propagation folds: geometry, kinematic evolution, and hydrocarbon traps. *Am Asso Petrol Geol Bull* 74:921–945
- Müller U (2004) Jung-Pleistozän–Eem–Warmzeit bis Weichsel-Hochglazial. In: Katzung G (ed) *Geologie von Mecklenburg–Vorpommern*. E. Schweizerbart'sche Verlagsbuchhandlung, Stuttgart, pp 234–242
- Müller U, Obst K (2006) Lithostratigraphie und Lagerungsverhältnisse der pleistozänen Schichten im Gebiet von Lohme (Jasmund/Rügen). *Z Geol Wiss* 34:39–54
- Mueller K, Suppe J (1997) Growth of Wheeler Ridge anticline, California: geomorphic evidence for fault-bend folding behaviour during earthquakes. *J Struct Geol* 19:383–396. [https://doi.org/10.1016/S0191-8141\(96\)00112-5](https://doi.org/10.1016/S0191-8141(96)00112-5)
- Noble TE, Dixon JM (2011) Structural evolution of fold-thrust structures in analog models deformed in a large geotechnical centrifuge. *J Struct Geol* 33:62–77. <https://doi.org/10.1016/j.jsg.2010.12.007>
- Panzig W-A (1995) Zum Pleistozän Nordost-Rügens. In: Katzung G, Hüneke H, Obst K (eds) *Geologie des südlichen Ostseeraumes – Umwelt und Untergrund*. Terra Nostra, Schriften der Alfred-Wegener-Stiftung 6:177–200
- Pedersen SAS (2000) Superimposed deformation in glaciectonics. *Bull Geol Soc Den* 46:125–144
- Pedersen SAS (2005) Structural analysis of the Rubjerg Knude glaciectonic complex, Vendsyssel, northern Denmark. *Geol Surv Denmark Greenl Bull*. <https://doi.org/10.34194/geusb.v8.4848>
- Pedersen SAS (2014) Architecture of glaciectonic complexes. *Geosciences* 4:269–296. <https://doi.org/10.3390/geosciences4040269>
- Pedersen SAS, Boldreel LO (2017) Glaciectonic deformations in the Jammerbugt and glaciodynamic development in the eastern North Sea. *J Quat Sci* 32(2):183–195. <https://doi.org/10.1002/jqs.2887>
- Pedersen SAS, Gravesen P (2009) Structural development of Maglevandsfald: a key to understanding the glaciectonic architecture

- of Møns Klint. *Geol Surv Denmark Greenl Bull* 17:29–32. <https://doi.org/10.34194/geusb.v17.5007>
- Pedersen SAS, Møller I (2004) Prediction and risk evaluation of chalk cliff collapse: the PROTECT project. *Geol Surv Denmark Greenl Bull* 4:89–92. <https://doi.org/10.34194/geusb.v4.4793>
- Phillips ER (2018) Glacitectonics. *Past Glacial Environments*. In: Menzies J, van der Meer JJM (eds) *Past glacial environments*. Elsevier, pp 467–502. <https://doi.org/10.1016/B978-0-08-100524-8.00014-2>
- Plonka N, Kenzler M, Hüneke H (2021) Syn-kinematic sedimentation between ice margin-parallel thrust-bounded ridges of the Glacitectonic Complex of Jasmund (Rügen Island, SW Baltic Sea, Weichselian). *Quat Int*. <https://doi.org/10.1016/j.quaint.2021.02.040>
- Rinterknecht V, Börner A, Bourlès D, Braucher R (2014) Cosmogenic  $^{10}\text{Be}$  dating of ice sheet marginal belts in Mecklenburg–Vorpommern, Western Pomerania (northeast Germany). *Quat Geochronol* 19:42–51. <https://doi.org/10.1016/j.quageo.2013.05.003>
- Slater G (1927) The structure of disturbed chalk and diluvium on the east coast of the Isle of Rügen (Jasmund District), Germany. In: *Report of the British Association*, 320–321
- Steinich G (1972) Endogene Tektonik in den Unter-Maastricht-Vorkommen auf Jasmund (Rügen). *Geologie* 20(Supplement 71/72):1–207
- Steinich G (1992) Die stratigraphische Einordnung der Rügen-Warmzeit. *Z Geol Wiss* 20:125–154
- Suppe J (1985) *Principles of structural geology*. Prentice-Hall, Englewood Cliffs, New Jersey
- van der Wateren FM (2003) Ice-marginal terrestrial landsystems: southern Scandinavian ice sheet margin. In: Evans DJA (ed) *Glacial landsystems*. Arnold, London, pp 166–203
- Vaughan-Hirsch DP, Phillips ER (2017) Mid-Pleistocene thin-skinned glaciectonic thrusting of the Aberdeen Ground Formation, Central Graben region, central North Sea. *J Quat Sci* 32(2):196–212. <https://doi.org/10.1002/jqs.2836>
- von Bülow K (1955) Stapelmoränen und Untergrund im norddeutschen Jungdiluvium. *Geologie* 4:3–14
- Winsemann J, Koopmann H, Tanner DC, Lutz R, Lang J, Brandes C, Gaedicke C (2020) Seismic interpretation and structural restoration of the Heligoland glaciectonic thrust-fault complex: implications for multiple deformation during (pre-) Elsterian to Warthian ice advances into the southern North Sea Basin. *Quatern Sci Rev* 227:106068. <https://doi.org/10.1016/j.quascirev.2019.106068>
- Ziesch J, Tanner DC, Krawczyk M (2014) Strain associated with the fault-parallel flow algorithm during kinematic fault displacement. *Math Geosci* 46:59–73. <https://doi.org/10.1007/s11004-013-9464-3>